



Modeling and Analysis of Permanent Magnet Synchronous Motors for Various Rotor Configurations

著者	Tong Yi, Morimoto Shigeo, Takeda Yoji, Hirasa Takao
引用	Bulletin of University of Osaka Prefecture. Series A, Engineering and natural sciences. 1991, 40(1), p.9-18
URL	http://doi.org/10.24729/00008410

Modeling and Analysis of Permanent Magnet Synchronous Motors for Various Rotor Configurations

Yi TONG*, Shigeo MORIMOTO**, Yoji TAKEDA** & Takao HIRASA**

(Received June 15, 1991)

Abstract—This paper presents a model of permanent magnet synchronous motors including motor losses and machine saliency. Base on this model, a maximum efficiency control algorithm is proposed for various types of PM motors. The efficiency is greatly improved by this control method. The efficiency characteristics are affected by the machine saliency which depends on rotor configuration and permanent magnets arrangement. The efficiency characteristics are examined in detail by the computer simulations and experimental results. A determination of the machine parameters is also described.

1. Introduction

Permanent magnet (PM) synchronous motors are showing increasing popularity in recent years for industrial drive applications. Since the lack of slip rings loss, brushes and field winding loss, the PM motor can offer significant efficiency advantages over induction and DC machines in adjustable-speed drives. Although the PM motor has inherently high efficiency, the efficiency depends on the control methods and the machine saliency. In addition, with the compact and slim rotor construction, very high-speed PM motors are easily designed. Since the operating speed and frequencies are high, core losses become very large and the efficiency grows worse¹⁾. Many PM motors are controlled by an $i_d=0$ control method, where the direct axis component of the armature current is not exist. This control method commonly used, because of its avoiding a demagnetizing action for the permanent magnets and linear relationship between armature current and torque. This control method, however, does not minimize the copper loss and the core loss. The recent development of the permanent magnets has brought materials with high coercivity and residual magnetism. Several current vector control methods are investigated to improve the performance of the PM motor by actively controlling the d-axis current²⁾. The performance characteristics are also affected by the machine saliency which depends on rotor configuration and permanent magnets arrangement³⁾⁻⁵⁾. This paper investigates the influence of the motor saliency and control methods on their efficiency characteristics.

* Graduate Student, Department of Electrical Engineering, College of Engineering.

** Department of Electrical Engineering, College of Engineering.

2. Modeling of PM Motors

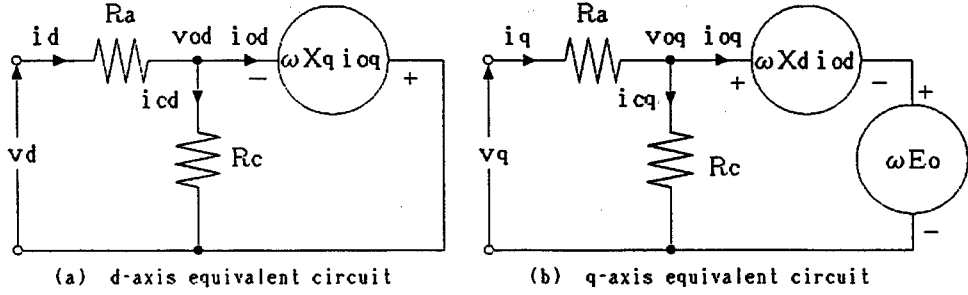


Fig. 1. d- and q-axis equivalent circuits of PM motor.

Fig. 1 shows the d- and q-axis equivalent circuits in the synchronously rotating reference frame, which include the effects of motor losses⁶⁾. All the parameters of this model are presented in per unit form expression. The major electrical losses in PM motors are the stator copper loss and the core loss. The copper loss is represented by resistance R_a and the core loss is represented by the shunt resistance R_c . The basic equations of the PM motor are then written as follows

$$\begin{pmatrix} v_d \\ v_q \end{pmatrix} = R_a \begin{pmatrix} i_{od} \\ i_{oq} \end{pmatrix} + (1 + R_a/R_c) \begin{pmatrix} v_{od} \\ v_{oq} \end{pmatrix} \quad (1)$$

$$\begin{pmatrix} v_{od} \\ v_{oq} \end{pmatrix} = \begin{pmatrix} 0 & -\omega\rho X_d \\ \omega X_d & 0 \end{pmatrix} \begin{pmatrix} i_{od} \\ i_{oq} \end{pmatrix} + \begin{pmatrix} 0 \\ \omega E_o \end{pmatrix} \quad (2)$$

where,

$$i_{od} = i_d - i_{cd}, \quad i_{oq} = i_q - i_{cq}$$

i_d, i_q : d- and q-axis components of armature current

i_{cd}, i_{cq} : d- and q-axis components of the core loss current

v_d, v_q : d- and q-axis components of armature voltage

X_d, X_q : d- and q-axis reactances

ρ : salient coefficient ($= X_q/X_d$)

E_o : open circuit voltage at rated speed

R_a : stator winding resistance per phase

R_c : core loss resistance

ω : electrical angular velocity.

The armature current I_a , the terminal voltage V_a and the torque T are expressed as follows

$$I_a = \sqrt{i_d^2 + i_q^2} \quad (3)$$

$$V_a = \sqrt{(R_a i_d - \omega X_q i_{oq})^2 + \{R_a i_q + \omega(E_o + X_d i_{od})\}^2} \quad (4)$$

$$T = \{E_o + (1 - \rho)X_d i_{od}\} i_{oq}. \quad (5)$$

In torque equation (5), the first term represents the magnet torque and the second term is recognized as the reluctance torque.

The copper loss W_{cu} , the core loss W_{fe} , the total electrical losses W_L and the efficiency η are expressed as follows

$$W_{cu} = R_a(i_d^2 + i_q^2) = R_a I_a^2 \tag{6}$$

$$W_{fe} = \frac{(-\omega X_q i_{oq})^2}{R_c} + \frac{\omega^2 (E_o + X_d i_{od})^2}{R_c} \tag{7}$$

$$W_L = W_{cu} + W_{fe} \tag{8}$$

$$\eta = \frac{T\omega}{T\omega + W_L} \times 100(\%) \tag{9}$$

3. Various Rotor Configurations

The PM motor has various rotor configurations and permanent magnet geometries. The PM motor can be classified according to the salient coefficient ρ , which is the ratio of d- and q-axis reactance ($\rho = X_q/X_d$). Fig. 2 shows the typical rotor configurations. In the surface permanent magnet (SPM) motor (Fig.1 (a), (b)), the magnets may be placed on the surface of the rotor. In the interior permanent magnet (IPM) motor (Fig.1(c)), the magnets are buried within the rotor core. As a relative

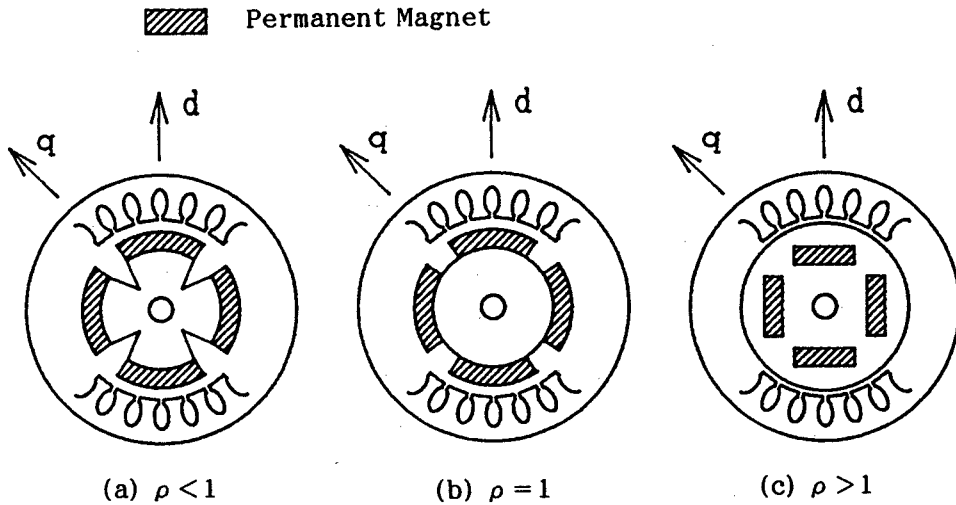


Fig.2. Cross section of PM motors.

((a), (b) : SPM machine, (c) : IPM machine)

permeability of the permanent magnet is very nearly unity, the magnet space behaves like an air. Therefore, the PM motor shown in Fig.1 (a) is a salient type machine ($\rho < 1$), and the surface PM motor shown in Fig.1 (b) is a nonsalient type machine ($\rho = 1$). On the other hand, the interior PM motor is a contrary salient type machine ($\rho > 1$).

4. Maximum Efficiency Control Algorithm

The efficiency can be improved more higher by actively controlling the d-axis current to minimize the total losses. The maximum efficiency control algorithm is found by differentiating the total losses W_L with respect to i_{od} .

$$i_{od} = -\frac{\omega^2 X_d E_o (R_a + R_c)}{R_a R_c^2 + \omega^2 X_d^2 (R_a + R_c)} \quad (10)$$

(for the nonsalient pole PM motor : $\rho = 1$)

$$T^2 = \frac{\{R_a R_c^2 i_{od} + (R_a + R_c)(X_d i_{od} + E_o)X_d \omega^2\} \{E_o + (1-\rho)X_d i_{od}\}^3}{\{(R_a + R_c)\omega^2 \rho^2 X_d^2 + R_a R_c^2\} (1-\rho)X_d} \quad (11)$$

(for the salient pole and contrary salient pole PM motor : $\rho \neq 1$)

The current i_{oq} is given as

$$i_{oq} = \frac{T}{\{E_o + (1-\rho)X_d i_{od}\}} \quad (12)$$

In practical control, the armature currents i_d and i_q are necessary.

$$i_d = i_{od} - \frac{\rho \omega X_d i_{oq}}{R_c}, \quad i_q = i_{oq} + \frac{\omega(E_o + X_d i_{od})}{R_c} \quad (13)$$

5. Losses and Efficiency

The parameter values for simulations are listed in table 1. The simulated motor is a contrary salient pole PM motor with $\rho = 2$.

Table 1. Parameters for simulations.

E_o	X_d	ρ	R_a	R_c
0.6	0.4	2	0.069	14

The core loss becomes dominant at high speeds. Fig. 3 shows the efficiency versus speed characteristics at rated torque by the $i_d = 0$ control method and the maximum efficiency control method. In the conventional $i_d = 0$ control, d-axis current i_d is

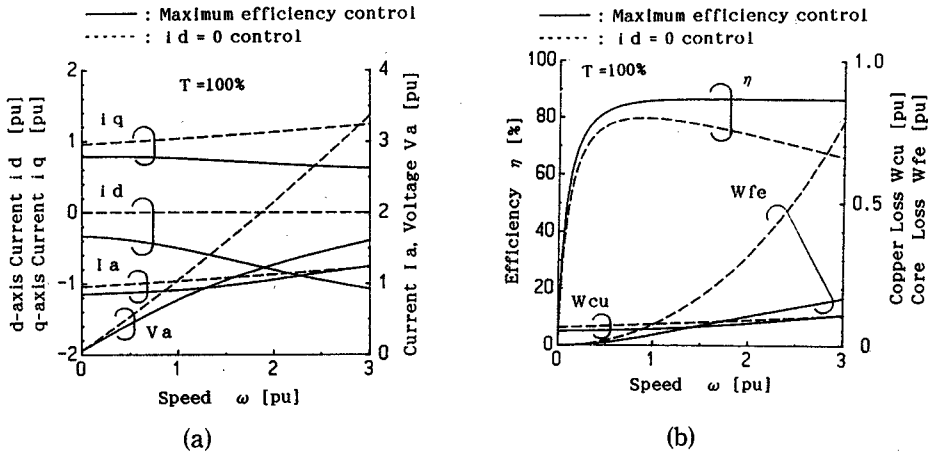


Fig. 3. Comparative performance of PM motor at rated torque ($T = 100\%$).

always kept zero. The copper loss remains relatively constant due to the constant torque. The core loss W_{fe} , which is proportion to voltage squared, increases significantly as the speed increases. Therefore, the efficiency becomes lower as increasing speed. On the other hand, d- and q-axis currents are controlled by Eqs. (11)–(13) in the maximum efficiency control. As the reluctance torque contributes to the total torque by the maximum efficiency control, the torque per I_a is larger and copper loss per torque becomes smaller than that of the $i_d = 0$ control method. In addition, the core loss becomes smaller since the terminal voltage is reduced by the d-axis armature reaction. At high speeds, the d-axis armature reaction reduces the core loss significantly then the efficiency is improved remarkably.

Fig. 4 shows efficiency and loss versus rotor saliency at rated speed and rated

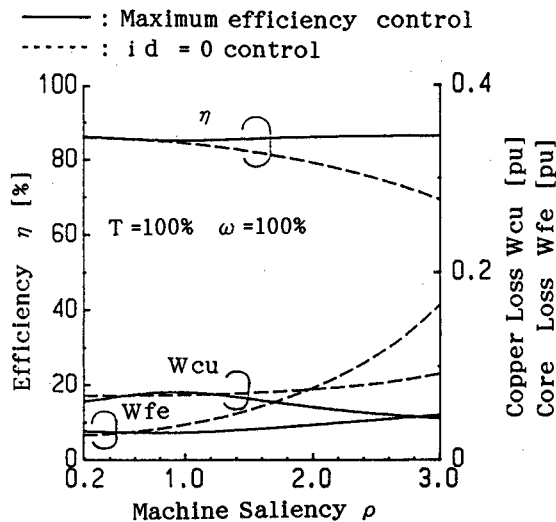


Fig. 4. Efficiency and loss versus machine saliency characteristics at rated speed and rated torque.

torque. The efficiency and core loss of the $i_d=0$ control method is greatly dependent on the motor saliency. Those of the maximum efficiency control method, however, independent on the motor saliency and remains nearly constant value. For the $i_d=0$ control, due to large q-axis armature reaction, the efficiency decreases with increasing saliency ρ . Fig. 5 shows the simulation results at high speed ($\omega=200\%$) and 50% torque. The more significant effect is obtained by the maximum efficiency control.

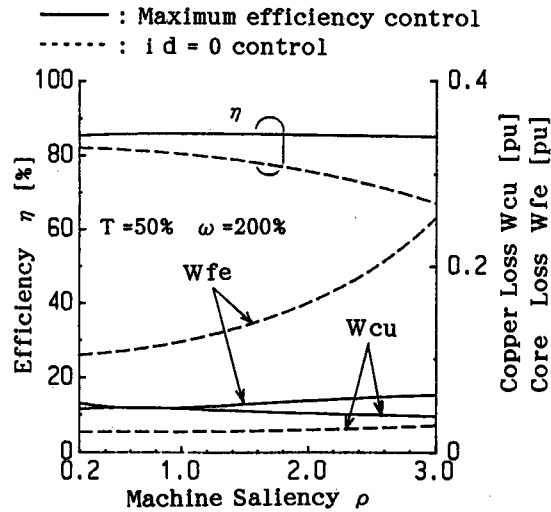


Fig. 5. Efficiency and loss versus machine saliency characteristics at 200% speed and 50% torque.

6. Determination of Parameters

Fig. 6 shows the scheme of the control system and measuring equipments. The

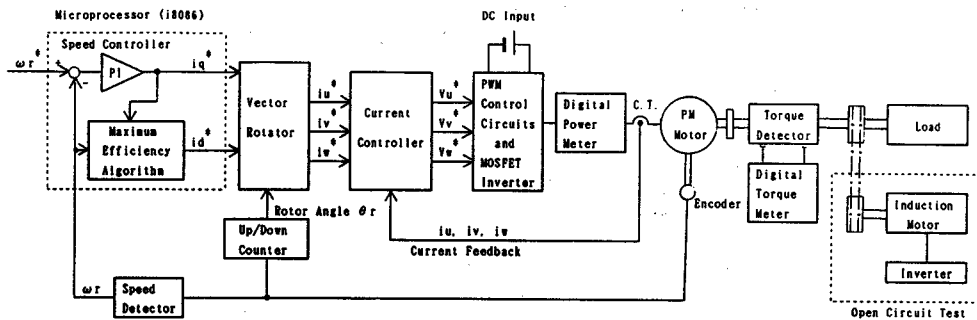


Fig. 6. Control system and measuring equipment.

equivalent circuit parameters for the PM motor can be determined by appropriate laboratory tests. The relationships between real unit and per unit are

$$\psi_a = E_o V_a^r, \quad L_d = X_d V_a^r / I_a^r, \quad L_q = X_q V_a^r / I_a^r$$

where, r represents rated values.

The stator resistance R_a should be measured immediately by means of a DC bridge after the heat-run operation. The stator windings are Y-connected, then half of the average line-to-line resistance gives R_a .

The PM motor is driven by an induction motor for open circuit condition. Measurement of the open circuit voltage determines the value of the flux linkage ψ_a .

Fig. 7 shows the torque versus speed characteristics under open circuit condition. The core loss resistance is evaluated by measuring the torque required to drive the PM motor as generator. The equivalent circuit model indicates that the armature current is zero and the power dissipated in the core loss resistance and friction is $\omega \cdot T_{mec} + V_o^2 / R_c$. The friction torque T_{mec} may be regarded as constant. The shaft torque will therefore be proportional ω and the slope of the speed-torque characteristics is R_c .

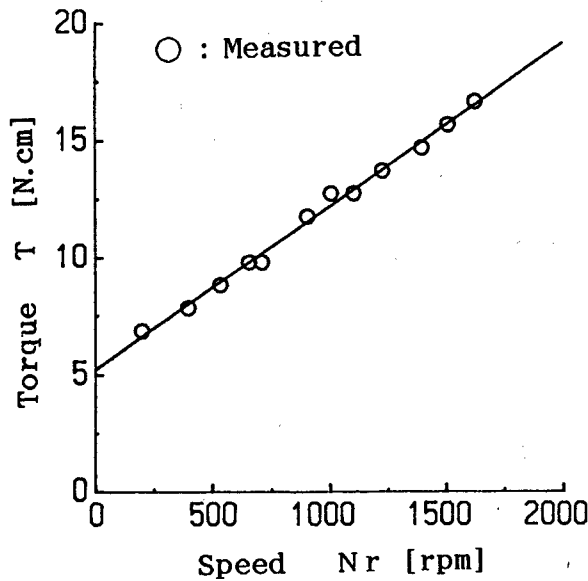


Fig. 7. Torque versus speed at open circuit test.

The d- and q-axis inductance may be calculated at any operating point through the following expressions obtained by the stator voltage equations which neglect the R_c . These measured inductances include the effect of the stator leakage inductances.

$$L_d = \frac{v_q - R_a i_q - \omega \psi_a}{\omega i_d} \quad (14)$$

$$L_q = \frac{R_a i_d - v_d}{\omega i_q} \quad (15)$$

The measured parameter values for the tested machine are listed in the table 2.

Table 2. Specifications and measured parameters of tested PM motor.

Output(W)	400
Rated speed (r/min)	1000
Rated current(A/rms)	5.0
Poles	4
$R_a(\Omega)$	0.98
$R_c(\Omega)$	400
$\psi_a(\text{Wb})$	0.26
$L_d(\text{mH})$	9.09
$L_q(\text{mH})$	18.1
$T_{\text{mec}}(\text{Nm})$	0.052

7. Experimental Results

The control system consists of the speed and current controllers, current sensors, optical encoder and a voltage source MOSFET inverter as shown in Fig. 6. The q-axis armature current command i_q^* (* represents the commanded value) is calculated by the proportional-integral (PI) compensation from the difference between the speed command ω_r^* and the detected speed ω_r . The d-axis armature current command i_d^* is calculated by the foregoing maximum efficiency algorithm.

Fig. 8 shows the experimental characteristics of the maximum efficiency control

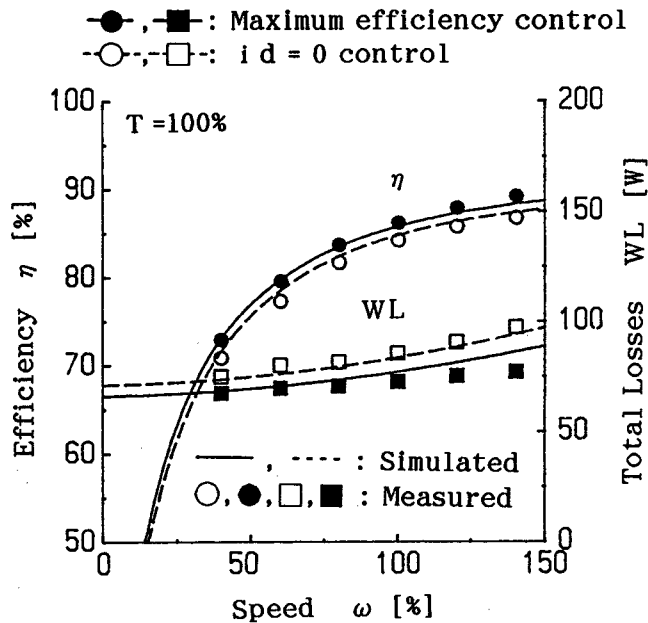


Fig. 8. Experimental efficiency and losses versus speed characteristics at rated torque.

and the $i_d=0$ control at rated torque. Due to the low operating speed, the efficiency is improved mostly by the reluctance torque. The experimental results agree well with the theoretical ones.

Fig. 9 shows the experimental efficiency characteristics at rated speed. At large torque, the measured efficiency is somewhat lower than the simulation results. One possible reason of this difference is the magnetic saturation. Although the core loss in the tested PM motor is a less significant, as reflected in the core loss resistance R_c , the improvement of the efficiency is confirmed.

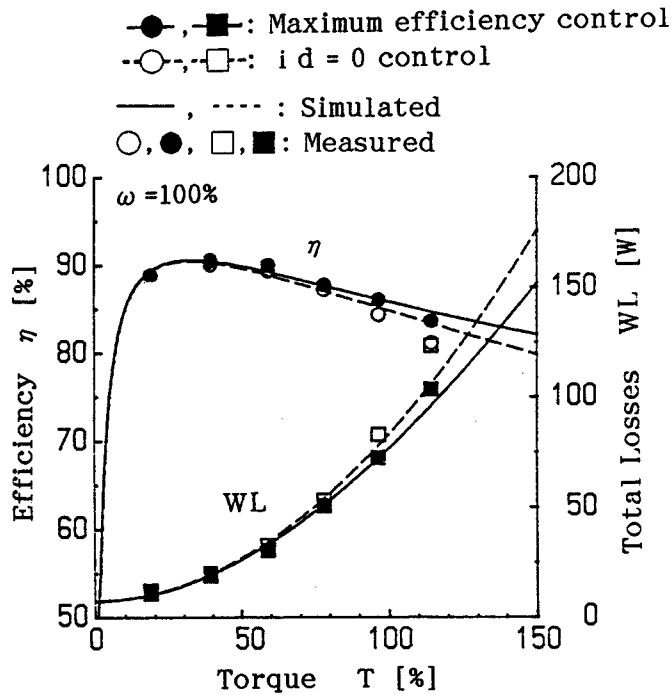


Fig. 9. Experimental efficiency and losses versus torque characteristics at rated speed.

8. Conclusion

The d-q axis model of the PM motor considering motor saliency and losses is sufficient for accurate modeling of the PM motors. The proposed maximum efficiency control is suitable for various types of PM motors, not only for the surface magnet PM motor, but also for the interior magnet PM motor. The efficiency is improved significantly by the maximum efficiency control method compared with the $i_d=0$ control method. The efficiency of the $i_d=0$ control method is greatly dependent on the motor saliency. In contrast, the efficiency of the maximum efficiency control method is independent of the motor saliency. Machines with large machine saliency ρ and small R_c more greatly effect can be obtained.

9. References

- 1) T. Sawahata, M. Miyagawa, H. Itoh, Y. Morimoto, T. Shimasaki, National Technical Report vol. 33, no. 5, pp. 79-87, Oct. 1987
- 2) S. Morimoto, Y. Takeda, T. Hirasa, IEEE Trans. Power Electron. vol. 5, pp. 133-139, Apr. 1990
- 3) R. F. Schiferl, T. A. Lipo, IEEE Trans. Ind. Appl., vol. IA-26, no. 1, pp. 115-123, Jan./ Feb. 1990
- 4) T. Sebastian, G. R. Slemon, IEEE Trans. Magnetics, vol. 22, pp. 1069-1071, Sep. 1986
- 5) S. Morimoto, Y. Takeda, T. Hirasa, K. Taniguchi, IEEE Trans. Ind. Appl., vol. IA-26, no. 3, pp. 866-871, Sep./ Oct. 1990
- 6) Y. Tong, S. Morimoto, Y. Takeda, T. Hirasa, BULLETIN OF UNIVERSITY OF OSAKA PREFECTURE, Series A ENGINEERING and NATURAL SCIENCES. vol. 39, no. 1, pp. 29-37, 1990